Environmental Microbiology (2018) **20**(8), 2898–2912 doi:10.1111/1462-2920.14273

Transcriptional responses of the marine green alga *Micromonas pusilla* and an infecting prasinovirus under different phosphate conditions

Charles Bachy,[1] Christina J. Charlesworth,[2†] Amy M. Chan,[2] Jan F. Finke,[2] Chee-Hong Wong,[3] Chia-Lin Wei,[3] Sebastian Sudek,[1] Maureen L. Coleman,[4] Curtis A. Suttle[2,5,6] and Alexandra Z. Worden[1,5*]

[1]*Monterey Bay Aquarium Research Institute, Moss Landing, CA 95039, USA.*

[2]*Department of Earth, Ocean and Atmospheric Sciences, University of British Columbia, Vancouver, BC V6T 1Z4, Canada.*

[3]*Lawrence Berkeley National Laboratory, Sequencing Technology Group, Joint Genome Institute, Walnut Creek, CA 94598, USA.*

[4]*Department of the Geophysical Sciences, University of Chicago, Chicago, IL 60637, USA.*

[5]*Integrated Microbial Biodiversity Program, Canadian Institute for Advanced Research, Toronto, M5G 1Z8, Canada.*

[6]*Departments of Botany, and Microbiology & Immunology, and Institute of Oceans & Fisheries, University of British Columbia, Vancouver, BC V6T 1Z4, Canada.*

Summary

Prasinophytes are widespread marine algae for which responses to nutrient limitation and viral infection are not well understood. We studied the picoprasinophyte, *Micromonas pusilla*, grown under phosphate-replete (0.65 ± 0.07 d^{-1}) and 10-fold lower (low)-phosphate (0.11 ± 0.04 d^{-1}) conditions, and infected by the phycodnavirus MpV-SP1. Expression of 17% of *Micromonas* genes in uninfected cells differed by >1.5-fold ($q < 0.01$) between nutrient conditions, with genes for P-metabolism and the uniquely-enriched Sel1-like repeat (SLR) family having higher relative transcript abundances, while phospholipid-synthesis genes were lower in low-P than P-replete. Approximately 70% (P-replete) and 30% (low-P) of cells were lysed 24 h post-infection, and expression of ≤5.8% of host genes changed relative to uninfected treatments. Host genes for CAZymes and glycolysis were activated by infection, supporting importance in viral production, which was significantly lower in slower growing (low-P) hosts. All MpV-SP1 genes were expressed, and our analyses suggest responses to differing host-phosphate backgrounds involve few viral genes, while the temporal program of infection involves many more, and is largely independent of host-phosphate background. Our study (i) identifies genes previously unassociated with nutrient acclimation or viral infection, (ii) provides insights into the temporal program of prasinovirus gene expression by hosts and (iii) establishes cell biological aspects of an ecologically important host-prasinovirus system that differ from other marine algal-virus systems.

Received 21 December, 2017; revised 6 April, 2018; accepted 7 May, 2018. *For correspondence. E-mail azworden@mbari.org; Tel. (+001) 831 775 2122; Fax (+001) 831 775 1620. †Present address: Center for Health Systems Effectiveness, Oregon Health & Science University, Portland, OR, USA

Introduction

Members of the genus *Micromonas* are motile unicellular prasinophytes that are among the most ecologically successful marine eukaryotic picophytoplankton (≤2 μm diameter), see, e.g. (Worden and Not, 2008; Massana, 2011). Little is known about how biotic (e.g., viruses) and abiotic (e.g., nutrients) factors influence growth and mortality of members of this diverse genus. Of note, the first virus isolated for a marine phytoplankter infects *Micromonas pusilla* (Mayer and Taylor, 1979). Since then, morphologically similar viruses infecting other *M. pusilla* strains have been isolated and shown to be common (Cottrell and Suttle, 1991, 1995). Between two and 10% of *Micromonas* cells are estimated to be lysed per day in the field (Cottrell and Suttle, 1995) and lysis can release about 70 infective particles per cell (Waters and Chan, 1982). Viruses have also been isolated that infect other *Micromonas* species (Maat *et al*., 2014; Baudoux *et al*., 2015). Collectively, these viruses are termed prasinoviruses and belong to a family of large double-stranded

DNA viruses, the *Phycodnaviridae* (Chen and Suttle, 1996). Prasinoviruses that infect *Bathycococcus* and *Ostreococcus*, which are close relatives of *Micromonas*, have also been described (Bellec *et al*., 2009; Moreau *et al*., 2010; Derelle *et al*., 2015). Analyses of marine samples using various approaches, including metagenomic sequencing, have demonstrated that such prasinoviruses are commonly present in surface ocean waters (Culley *et al*., 2009; Monier *et al*., 2012).

Despite their widespread occurrence and apparent ecological significance, the interactions of prasinoviruses with their hosts have yet to be characterized at the molecular level. The availability of genome sequences from several *Bathycoccus* and *Ostreococcus* viruses (Moreau *et al*., 2010; Derelle *et al*., 2015), as well as four *Micromonas* viruses, including MpV-SP1 (Finke *et al*., 2017b) poise the field for such studies. These prasinoviruses have similar genome sizes and a core set of shared genes that includes several host-derived auxiliary metabolic genes (AMGs) (Monier *et al*., 2017), as well as a large pangenome. Despite these considerable genomic resources, variation in expression of viral genes during the lytic cycle remains unexplored in prasinoviruses. The only expression study thus far used qPCR to determine that copies of the MpV-SP1 *polB* gene increased during the infection time course while *M. pusilla* 18S rRNA copies decreased. These results were interpreted as suggesting that an accumulation of viral genomes occurred at the expense of host DNA synthesis toward the end of the lytic cycle (Brown *et al*., 2007).

The *Micromonas* genus itself harbors considerable diversity. Of the seven distinct *Micromonas* clades, Clades A, B, and C (*sensu* Simmons *et al*., 2015) are closely related and are represented by the genome-sequenced species *Micromonas commoda* (RCC299). Clades E1 and E2 branch adjacent to one another, with E2 being a high latitude/polar species, *Micromonas polaris* (Simmons *et al*., 2015; Simon *et al*., 2017). There is one as yet uncultured group, *Micromonas* Clade _.IV (Worden, 2006). Clade D contains the genome-sequenced species *Micromonas pusilla* (CCMP1545, Clade D *sensu* Simmons *et al*., 2015) which can be infected by the MpV-SP1 virus, the type species of the genus *Prasinovirus* (King *et al*., 2012). The *Micromonas* clades show extensive divergence (Guillou *et al*., 2004; Šlapeta *et al*., 2006; Simmons *et al*., 2015), such that *M. pusilla* and *M. commoda* share only 80% of their protein encoding genes (Worden *et al*., 2009; van Baren *et al*., 2016). Not surprisingly, viruses isolated against *M. pusilla* do not infect members of the other *Micromonas* clades, and infectivity appears to even be limited to specific strains within *Micromonas* Clade D (Bellec *et al*., 2014; Baudoux *et al*., 2015). The distribution and ecological importance of the different *Micromonas* clades, alongside availability of complete genome sequences for two species (van Baren *et al*., 2016), transcriptome assemblies for all but the uncultured clade (Keeling *et al*., 2014), and genomes from several viruses (Moreau *et al*., 2010; Finke *et al*., 2017b), make the *Micromonas*/prasinovirus system both tractable and environmentally relevant.

In many marine environments, abiotic factors, especially nutrient availability, play important roles in regulating phytoplankton growth and primary production rates (Field *et al*., 1998). For example, in the Sargasso Sea where *Micromonas* is observed at higher abundances in winter and spring than summer, increased stratification and phosphate limitation during summer are linked to reduced contributions by eukaryotic phytoplankton and dominance by the cyanobacterium *Prochlorococcus* (Treusch *et al*., 2012). The extent of phosphate limitation in both the Sargasso and Mediterranean Seas also appears to manifest in gene content of cyanophages (Sullivan *et al*., 2005), where phosphate-acquisition related genes are enriched relative to those in cyanophages from the Pacific Ocean (Kelly *et al*., 2013). Further, in a *Prochlorococcus*-cyanophage system, transcript levels of P-transport-related phage genes are elevated in P-starved hosts relative to P-replete hosts (Zeng and Chisholm, 2012; Lin *et al*., 2016). In prasinoviruses, both phosphate (Monier *et al*., 2012) and ammonium transporters (Monier *et al*., 2017) have been reported. Thus, it has been inferred that the virus (or cyanophage) may induce increased host uptake of the particular nutrient during infection. This has been shown for a virally-encoded ammonium transporter expressed and utilized by the host, *Ostreococcus tauri*, during infection (Monier *et al*., 2017), but has not yet been demonstrated for eukaryotic-virus phosphate transporters. Rather, evidence for the influence of phosphate in host-virus interaction is based on viruses being thought to have relatively high phosphate requirements (Jover *et al*., 2014), and the idea that phosphate availability limits viral production, infection kinetics, and burst size, as well as host growth rates (Gunnar Bratbak *et al*., 1996; Wilson *et al*., 1996; Maat *et al*., 2014). Eukaryotic host-virus dynamics under varying nutrient levels have been studied in Clade C *Micromonas* LAC38 (Maat *et al*., 2014; 2016b,c). The LAC38 strain has 100% 18S rRNA identity to *Micromonas* Clade C strains and is phylogenetically closer to Clade A species *M. commoda* than to Clade D species *M. pusilla* (as which LAC38 was originally misidentified). In the studies of Maat and colleagues, a prasinovirus of LAC38 exhibited a longer latent period and lower viral production in hosts grown under phosphate deplete conditions, relative to replete conditions, similar to differences observed under varying nitrogen availability (Maat and Brussaard, 2016).

The influence of nutrient availability on growth of hosts and viral replication have yet to be examined

alongside corresponding transcriptional responses in marine eukaryotic phytoplankton-virus systems. Here, we investigated the influence of phosphate availability on the growth and transcriptomic responses of *M. pusilla* (CCMP1545), in the presence or absence of infection by the prasinovirus MpV-SP1. In addition to flow cytometric analyses of virus and host populations, RNA-seq samples were collected 1.5, 3 and 12 hr after initiation of the infection experiment and sequenced. The resulting transcripts were mapped to the host and virus genomes and differential expression was analyzed. The design of the study allowed us to examine how relative transcript abundances differed in both *M. pusilla* and the virus under replete and low-phosphate conditions. Collectively, these studies provide first insights into the transcriptional program of a virus after infecting a eukaryotic picophytoplankton species.

Results and discussion

Host cell growth rates and viral infection dynamics

Micromonas exhibits marked synchronized differences in gene expression profiles (Waltman *et al*., 2016), as well as chlorophyll fluorescence and cell size, over the cell-cycle when grown under a light:dark cycle (Jacquet *et al*., 2001; DuRand *et al*., 2002; Cuvelier *et al*., 2017). Here, experiments were performed under continuous light to avoid the influence of cell-cycle synchronization, which would differ in a growth-rate dependent manner between our treatments. Further, little is known about how viral entrance into the cell, and viral infection kinetics are influenced by the host-cell-cycle phase. Hence, here, use of unsynchronized cultures (i.e., continuous light) was important for focusing on the effects of nutrient status on hosts and viral infection, as done in other phytoplankton RNA-seq studies on nutrient limitation (see e.g., Bender *et al*., 2014). Lack of synchronization was manifested in *M. pusilla* population mean forward angle light scatter (FALS, a rough indicator of cell size) being constant over the RNA-seq time course (ending at T12) and cell abundance increasing incrementally (Supporting Information Fig. S1), unlike patterns observed for synchronized *M. commoda* cells over a similar timeframe (Cuvelier *et al*. 2017). Growth rates of *M. pusilla* over the 24-h experimental period differed between P-replete conditions (0.65 ± 0.07 d^{-1}, ~one doubling every 24 h) and slower growing low-P cells (0.11 ± 0.04 d^{-1}, $p < 0.001$; Fig. 1A), reflecting an 83% reduction in growth rate between the uninfected P-replete and low-P treatments.

Cells in treatments with added viruses died at both levels of phosphate availability (as manifested by the 'negative' growth rates computed for infected cultures, Fig. 1A), as expected. Viral particles were also enumerated using flow cytometry and SybrGreen staining (Payet and Suttle, 2008; Brussaard *et al*., 2010). These results demonstrated that after 12 hours extracellular viral particles had increased by $79 \pm 36\%$ in the P-replete conditions from T0 values and by $8 \pm 8\%$ in the low-P treatment. This difference persisted such that 24 h after infection the number of viruses released in the P-replete treatment was still higher than in the low-P treatment ($p < 0.01$) (Fig. 1B). Further, while *Micromonas* abundance during infection was not different between the replete and low-P treatments at T12 (*t*-test; $p = 0.86$), at T24 they were significantly lower in P-replete ($1.0 \pm 0.1 \times 10^6$ ml^{-1}) than low-P ($2.1 \pm 0.1 \times 10^6$ ml^{-1}; *t*-test, $p < 0.001$).

In a prior study, chlorophyll-pigmented particles observed during an algal viral lysis event that scattered less light than the alga itself were inferred to be chloroplasts released from lysed host cells into the medium

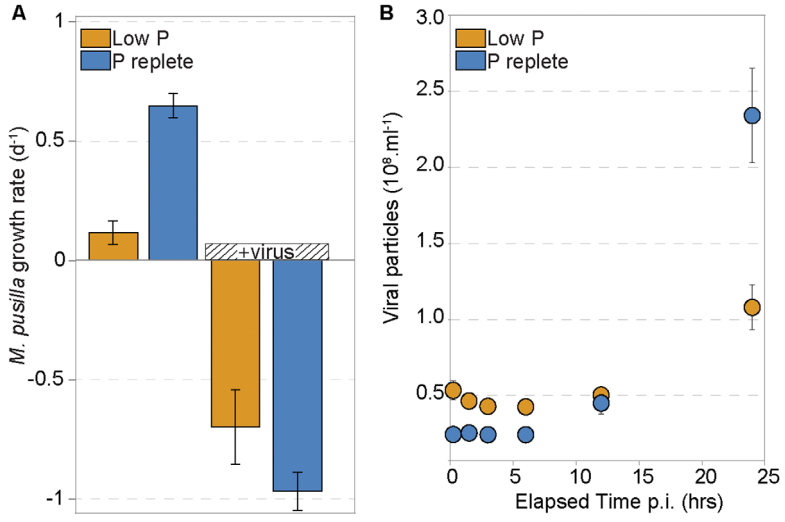

Fig. 1. Growth of *Micromonas pusilla* and production of viruses under experimental treatments measured from biological triplicates.
A. Daily growth rate measured over 24 h of *M. pusilla* cultures in replete (25 μM) and low (2.5 μM) P medium under continuous light.
B. MpV-SP1 particles enumerated by flow cytometry over the time course in infected *M. pusilla* cultures acclimated to replete- and low-P conditions. Shown are the mean and standard deviation of biological triplicates for each condition.

(Brown and Bidle, 2014). This conclusion was made after tests using various stains to distinguish intact hosts from lysing hosts, and the much smaller particles, which were presumed to be free chloroplasts (post lysis) in flow cytometric analyses of infected cultures of *Aureococcus anophagefferens.* Although the host genera *Micromonas* and *Aureococcus* belong to different eukaryotic supergroups (Adl *et al*., 2012), the virus isolates AaV and MpV-SP1 are both Nucleocytoplasmic Large DNA Viruses (NCLDVs), and would be expected to cause cell lysis in a similar manner (Moniruzzaman *et al*., 2014). Hence, assuming that chlorophyll-pigmented particles with much lower light scatter than *M. pusilla* cells also reflect free-chloroplasts (and hence lysed cells, since each *Micromonas* has one plastid) in the algal system understudy here, we also estimated the proportion of lysed *M. pusilla* cells by flow cytometry. The free-chloroplast analysis indicated that at minimum 70% (P-replete) and 30% (low-P) of cells had lysed by 24 h after infection (Supporting Information Fig. S2), coinciding with the large increase in free virus particles (again larger for P-replete) observed using direct enumeration by SybrGreen staining and flow cytometry (Fig. 1B). The free-chloroplast numbers were lower than would be estimated based on the direct enumeration of changes in cell abundance, possibly due to rapid degradation of the free-chloroplasts (a degradation rate as yet unknown). Nevertheless, this analysis supports general trends on timing of reductions in algal cell abundance (Supporting Information Fig. S1) and increases in extracellular viral particle abundance (Fig. 1B). Overall, the results demonstrated that cells in the P-replete treatment produced more viral particles than the low-P treatment (Fig. 1B).

The lower viral production observed for *M. pusilla* cultures grown under reduced phosphate availability could be due to specific P-limitation of viral replication or to an indirect effect of host growth rate. Our results from the *M. pusilla*/MpV-SP1 host-virus system are similar to those from Clade C *Micromonas* strain LAC38 when infected by the virus MpV-08T. The latter phycodnavirus infects *Micromonas* Clade C, and potentially two Clade D members (RCC498 and RCC629), but not other Clade D members such as *M. pusilla* CCMP1545 (Martínez Martínez *et al*., 2015). In the LAC38/MpV-08T system the latent period was significantly longer in a phosphate-starved, nitrogen-starved and N-/P-starved treatments, and fewer viral particles (i.e., smaller burst size) were released from host cells (Maat *et al*., 2014) as compared to the replete infected control (batch experiments). In that study, pre-experiment LAC38 cultures were grown in semi-continuous mode, and exhibited similar growth rates across the nutrient limitation treatments and the control. However, unlike these pre-experiment cultures, the growth rate of nutrient-limited cultures dropped dramatically, in a uniform manner across limited treatments ($62 \pm 16\%$ lower than replete controls) once moved into the batch mode for the viral infection experiments. Likewise, when Clade C *Micromonas* strain LAC38 was subjected to reduced light, the burst size of MpV-08T was reduced and the latent period extended (Maat *et al*., 2016c). Further, optimal viral replication (i.e., shortest latent period and fastest viral production) appears to occur at the temperature supporting maximum host growth rate in *Micromonas* Clade E1 members (Demory *et al*., 2017). Collectively, these studies point to dependence of viral production and lysis rates on host growth rate, or growth-rate-associated factors (e.g., reduced numbers of ribosomal RNAs/translation machinery), but independent of the rate-limiting growth factor or the specific host-virus system understudy.

Gene expression of M. pusilla *cells acclimated to replete- and low-P conditions*

We compared transcriptomes of uninfected *M. pusilla* cultures in P-replete and low-P conditions to understand how phosphate availability influences cellular responses at the transcriptional level. Sequencing depth ranged from 46 to 78 million paired-end reads per sample (Table 1). Approximately 16.7% of the 9,870 protein-encoding genes in the 22 Mb *M. pusilla* genome showed differential expression (>1.5 FC, $q < 0.01$), between the phosphate treatments (Fig. 2). In low-P, 9.9% (979) of genes were more highly expressed than in P-replete, based on relative transcript abundance, while 6.8% (668) had lower expression (Supporting Information Table S1). Thus, 83.3% of the transcriptional program remained relatively stable between the two phosphate availability levels. These results are consistent with the level of transcriptional change in *M. commoda* when cultures acclimated to replete versus phosphate-limiting conditions are compared (Guo *et al*., 2018).

We next investigated a number of manually-annotated pathways that have been implicated in phytoplankton nutrient stress responses. Studies on P-starved marine algae from different eukaryotic supergroups than *Micromonas* (Dyhrman *et al*., 2006, 2012; Orchard *et al*., 2009; Wurch *et al*., 2014) and on non-marine plants and chlorophyte algae (Schachtman *et al*., 1998; Grossman and Aksoy, 2015), which are phylogenetically relatively close to *Micromonas*, emphasize the importance of phosphate in nucleic acids, membrane phospholipids and key metabolic processes. Here, several genes involved in phosphate transport, including three sodium-dependent phosphate symporters, two genes involved in polyphosphate accumulation and an unidentified ABC transporter (JGI ID 3412) showed significantly higher expression in low-P than P-replete conditions (Fig. 2). Similarly, phosphate transporters increased in P-

Table 1. Reads mapped to the host (*M. pusilla* CCMP1545) and virus (MpV-SP1) genomes over the experimental time course

Sample ID	*M. pusilla* genome	MpV-SP1 virus genome
P-Replete T1.5 hours	50,126,193 ± 1,150,141	n.d.
P-Replete T3 hours	48,157,836 ± 4,481,639	n.d.
P-Replete T12 hours	46,595,625 ± 3,700,142	n.d.
Infected P-replete T1.5 hours	49,215,922 ± 5,480,037	147,804 ± 9,088
Infected P-replete T3 hours	54,449,275 ± 2,953,263	341,875 ± 26,667
Infected P-replete T12 hours	47,534,416 ± 1,091,079	5,386,163 ± 123,930
Low-P T1.5 hours*	69,616,257	n.d.
Low-P T3 hours	49,164,231 ± 1,338,041	n.d.
Low-P T12 hours	55,488,577 ± 8,168,380	n.d.
Infected low-P T1.5 hours	49,109,379 ± 2,169,170	644,112 ± 12,479
Infected low-P T3 hours	64,961,297 ± 10,956,483	1,263,125 ± 216,011
Infected low-P T12 hours	50,190,309 ± 6,856,493	3,254,363 ± 832,675

Values shown represent the mean and standard deviation of biological duplicates. *, no replication due to sample loss during sequencing; n.d., not detectable.

deficient as well as P-limited cultures of *M. commoda* based on RNA-seq analyses (Whitney and Lomas, 2016; Guo *et al*., 2018), and in the green alga *Tetraselmis chui* using qPCR (Chung *et al*., 2003). Interpretation of metatranscriptomic studies of natural assemblages (Caron *et al*., 2017) will rely on understanding the extent to which these genes serve as absolute markers, or vary depending on the ratio of available N:P and other factors.

Land plants and bacteria (Minnikin *et al*., 1974; Dörmann and Benning, 2002), as well as marine cyanobacteria, stramenopiles and haptophytes (Van Mooy *et al*., 2009; Wurch *et al*., 2011), can substitute non-phosphorus lipids, such as sulfolipids, for phospholipid membranes when phosphorus is scarce. In P-limited chemostat conditions Clade C *Micromonas* strain LAC38 shows enrichment of non-phosphorus lipids relative to phospholipids (Maat *et al*., 2016a), when compared to replete conditions. Here, *M. pusilla* transcripts for three genes involved in phospholipid synthesis (JGI IDs 6624, 6786 and 8316) were significantly lower in low-P than P-replete, while phospholipase (responsible for phospholipid degradation; JGI ID 8414) was higher (Fig. 2). However, relative transcript abundances of *M. pusilla* genes involved in galactolipid (*DGD*, JGI ID 437 and *MGD*, JGI ID 4829) and sulfolipid (*SQD1*, JGI ID 699 and *SQD2*, JGI ID 6144) synthesis did not change significantly between the two phosphate conditions. Thus, the reduction of phospholipid machinery maybe more associated to reduced turnover that accompanies slower growth, than a massive change in lipid composition. Alternatively, other mechanisms for modulating synthesis rates, and/or the sulfolipid pathway, might play a role that obscures transcription level responses. For example, post-transcriptional processes are important in eukaryotes (Hanson and Coller, 2018), including *Micromonas* as shown in both diel and P-limitation experiments (Waltman *et al*., 2016; Guo *et al*., 2018), and thus often do not reflect changes at the protein level.

Other genes coding for proteins reported as being activated under P-stress, such as alkaline phosphatase, (e.g., JGI IDs 5187 and 5684 in *M. pusilla*) did not change significantly between the low-P and P-replete treatments. Finally, many of the other genes that showed higher (329 of the 979 that changed) or lower (185 of the 668 that changed) relative transcript abundance under the low-P conditions relative to P-replete have unknown functions. These genes may have important roles in P-acquisition or as yet unknown aspects of growth adjustment processes (see Supporting Information Tables S1 and S2).

General gene expression and functional enrichment analyses of infected and uninfected cells

We then examined changes in host gene transcript abundances in infected cells and how they connected to the differing phosphate supply levels (Supporting Information Table S2). Here, we were only able to work with duplicates for the RNA-seq analysis, and thus had reduced statistical power, potentially obscuring some changes. At a global level, pairwise comparisons between all treatments and time points through T12 showed that P-availability had a stronger impact on *M. pusilla* gene expression than did viral infection (Fig. 3A). On average 372 ± 326 *M. pusilla* genes had differentially expressed transcripts (3.8 ± 3.3% of genes in the genome, $q < 0.01$ and >1.5 fold change) between infected and uninfected cells for the same time point and the same P treatment. This is markedly lower than the 1741 ± 365 genes that showed differential expression between the uninfected low-P and P-replete treatments for the same time point. These findings may stem from dominance of the RNA-seq signal by transcripts from healthy, uninfected host cells. Alternatively, the distribution of our time points may have caused us to 'miss' the peak expression of genes influenced by infection. It is also possible however that the impact of viral infection on the overall host gene

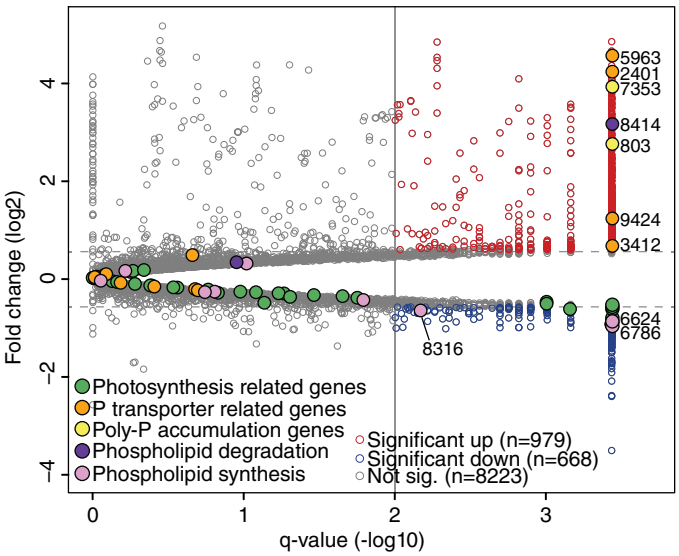

Fig. 2. Differential gene expression in *M. pusilla* grown under low- and replete-phosphate availability. The volcano plot showing fold-changes in transcript abundances for individual *M. pusilla* genes that are significantly ($q < 0.01$) enriched (red) or depleted (blue) in the low-P treatment compared to the P-replete treatment for uninfected cultures. Data from T1.5 and T3 were analyzed together for the low-P, and these time points were also combined for the replete-P since these cultures were grown under continuous light and therefore should be replicates for the uninfected cultures. This allowed us to compare quadruplicated transcriptomes of the low-P to the high-P treatments surmounting statistical issues created by sample loss in sequencing that resulted in only having duplicates from these time points. Larger and coloured circles (see legend) highlight representative genes encoding proteins from selected functionally annotated groups. The vertical grey line shows where $q = 0.01$ with points to the right of the line having $q < 0.01$ and points to the left of the line having $q > 0.01$. The horizontal dashed grey lines show fold-changes more or less than 1.5 (0.58 log2 FC). Numbers on the right side are locus tag as in JGI for differentially expressed genes mentioned in the main text.

expression is small relative to factors that control cell replication under different growth rates or nutrient conditions.

Functional enrichment analysis identified biological processes affected by phosphate availability in uninfected *M. pusilla* cells. Genes from five KOG classes were significantly enriched under P-replete conditions relative to low-P, specifically genes involved in translation, ribosomal structure and biogenesis, transport and metabolism of nucleotides and amino acids, RNA processing and modification, and finally, nuclear structure (Fig. 3B and Supporting Information Table S3). These reflect cellular modifications required to accomplish the faster growth rates seen in P-replete relative to low-P. In contrast, under low-P, genes for post-transcriptional modifications, signal transduction mechanisms, defense mechanisms or intracellular trafficking, secretion and vesicular transport were enriched (Fig. 3C). Those with the strongest enrichment signal belonged to the post-translational modification, protein turnover, chaperones KOG class which includes proteins with Sel1-like repeat (SLR) domains (Supplementary table S3). These SLR domain-containing proteins are unique to *Micromonas* and this gene family is greatly expanded in Clade D (*M. pusilla*) relative to Clade A (*M. commoda*) (van Baren *et al*., 2016). Twenty-nine out of the 80 SLR proteins in the *M. pusilla* genome (van Baren *et al*., 2016) showed increased relative transcript abundance with fold-changes > 4 in the low-P treatment. SLR gene activation has been observed under endoplasmic reticulum-stress-inducing conditions in other eukaryotes (Mittl and Schneider-Brachert, 2007), and one SLR protein controls extracellular matrix deposition during cell division in yeast (Oh *et al*., 2017), but otherwise their functions are not known. Ours is the first report of SLR transcriptional responses in phytoplankton and provides targets for future investigation of how cells modulate and modify division in response to changes in nutrients or potential stress factors. Overall, a number of the differentially enriched categories in replete and low-P cells are consistent with cellular modifications associated with changes in growth rate. Several of the specific host machinery components that showed enrichment would also influence viral replication rates, likely increasing them under the high growth conditions.

Comparison of infected and uninfected treatments showed significant enrichment of host genes in the KOG class for carbohydrate transport and metabolism at the final RNA-seq time point, T12, when cells were clearly infected (12 genes, Figs 1 and 3D and Supporting Information Table S3). The glycolysis pathway is the central pathway of carbohydrate metabolism, and here two genes annotated as FBPA-2 and GAPDH-4 showed significant enrichment (JGI 5173 and 4276 respectively) as did a phosphoglycerate mutase (JGI 422), two pyruvate kinases (JGI 9357 and JGI 9370) and a 3-phosphoglycerate kinase (JGI 8039) (Supporting Information Table S4). Consistent with increased expression of these glycolysis genes, two CAZymes, from different glycosyltransferase families (GT4/GT5 and GT25: JGI 1639 and 4373 respectively), were also among genes with significantly higher relative transcript abundance 12 h after infection. Host glycolysis is considered essential for virus production and in some cases, specifically in some mammals when infected by viruses, appears to be enhanced by the infection (see review in Sanchez and Lagunoff, 2015). Upregulation of glycolysis occurs during the early phase of viral infection in the haptophyte alga *Emiliania huxleyi* (Rosenwasser *et al*., 2014) – highlighting a potential similarity between two algal-virus systems involving hosts from distant algal lineages.

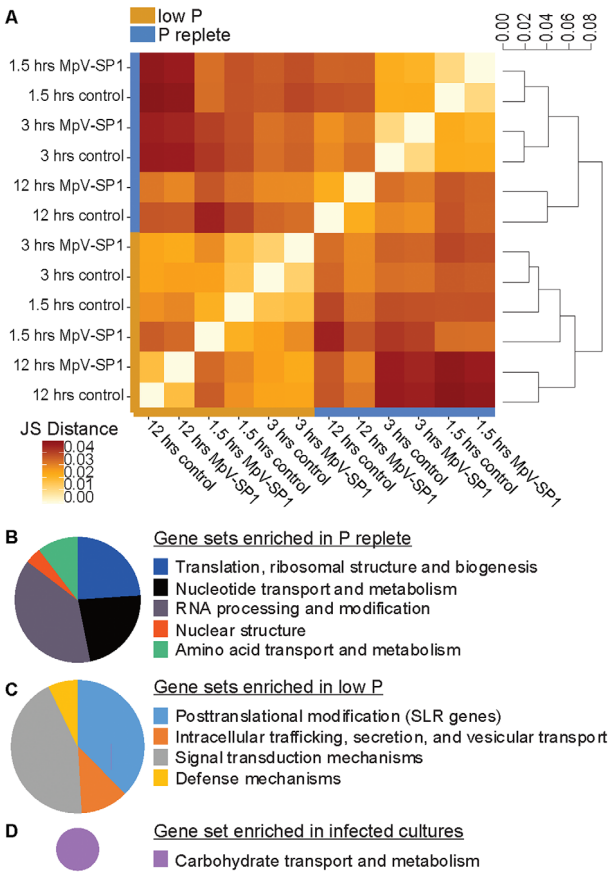

Fig. 3. Global changes in *M. pusilla* gene relative transcript abundances under different phosphate conditions and infection states.
A. Heat map showing the Jensen-Shannon (JS) distances of transcriptomes across all conditions with biological duplicates collapsed. Samples labelled + SP1 indicate those with the virus MpV-SP1 added at T0. The dendrogram (right) shows JS distances analyzing pattern of gene expression between treatments.
B and C. Host genes in significantly enriched KOG classes based on functional enrichment analysis (T1.5 and T3 analyzed together) for the uninfected cells in replete-P and low-P conditions respectively.
D. One KOG class was significantly enriched in infected host cells at T12, whereas at time points T1.5 and T3 no significant gene enrichments were observed and the infection was clearly in very early stages (Fig. 1). In (B, C, and D), only the host genes which showed significant ($q < 0.01$ and FC > 1.5) differential expression are displayed in the pie charts. The pie chart sizes are proportional to the number of genes included (total of 96, 112 and 12 genes in B, C and D respectively).

Once again, many other genes encoding proteins of unknown function had enriched (133 of the 431 that changed) or depleted transcript abundances (32 of the 145 that changed) in infected cells relative to control (i.e., uninfected) cells at T12. These uncharacterized genes likely have important roles in the general cellular responses to viral infection.

Genome-wide MpV-SP1 transcription

We also mapped the RNA-seq data to the genome of the 173-kb MpV-SP1 virus (Finke *et al*., 2017b) which contains 242 predicted protein-encoding genes. Fragments per kilobase per million mapped reads (FPKM) values were generated for all genes at each of the three time points in the replete and low-P treatments (Supporting Information Table S5). Overall, 99.9% of the virus genome sequence recruited transcripts at T12. The 0.1% that did not recruit reads was at the extremities of the genome, which is comprised of inverted terminal repeats. Transcripts from all 242 viral genes were detected in both the P-replete and low-P treatments. Ninety-three% of the nucleotides in the MpV-SP1 virus genome had previously been incorporated in gene models (GenBank accession PRJNA47589). The remaining 7% presumably corresponded to intergenic space, such that intergenic regions ranged from 1 to 724 bp (average 50 $\pm$ 91 bp). We observed that at T12, 4% of the transcript bases that aligned to the MpV-SP1 viral genome corresponded to intergenic regions, indicating that coding domain sequences had previously been underestimated. Based on our estimates the coding proportion of the MpV-SP1 genome is 95.99%, bringing this compact prasinovirus genome in line with other prasinoviruses, such as the *Ostreococcus* viruses (Derelle *et al*., 2015).

The proportion of viral transcripts increased in relation to the total mRNA pool over time in both phosphate treatments (Supporting Information Fig. S3). As mentioned above, *Micromonas* cellular abundances in the two treatments did not differ at T12, but proportionally more reads mapped to the virus in the P-replete treatment (10.18 $\pm$ 0.69% of the overall Illumina reads) than in the low-P treatment (6.04 $\pm$ 0.01%). Most probable number (MPN) assays were not performed, however, the host-cell density and the viral particle ratios were similar in both phosphate treatments, therefore host-virus encounter rates should be consistent between the different treatments. The lower proportion of virus:host reads in the low-P treatment could indicate that fewer cells were infected. However, it could also stem from lower host transcriptional activity (in low-P than P-replete), as indicated by our host RNA-seq enrichment analysis (Fig. 3B and C), in an equal number of infected cells, resulting in overall lower viral replication and proliferation in the low-P treatment.

MpV-SP1 expression program during infection of M. pusilla *under differing P availabilities*

The 50 most highly expressed viral genes were the same in both phosphate conditions (see Supporting Information Table S5) and most encode proteins of unknown function (80% lack Pfam domains). For those with functional annotations, six encode proteins that are likely involved in viral machinery for gene expression (RNAse III, general/initiation and elongation transcription factors and

mRNA capping enzyme) and four are probably involved in DNA replication (exonuclease, DNA polymerase IV, DNA ligase and helicase) (Table 2).

To investigate the possibility that some viral genes may be differentially transcribed by hosts grown under the two P-availability levels, we compared whole-genome viral expression profiles for each time point in low- and P-replete conditions. Of 242 predicted genes in the MpV-SP1 genome, 8 (T1.5), 9 (T3) and 8 (T12) were differentially expressed when comparing infection of low-P with P-replete acclimated host cells at each time point (Fig. 4). Most of these transcripts encoded proteins of unknown function. The exceptions were MPXG_00046 (helicase/NTPase) for which the relative transcript abundance was higher at T1.5 (1.9-fold change) under low-P, and MPXG_00234 (helicase) with a lower relative transcript abundance at T12 under low-P than P-replete. In addition, two of the eight capsid proteins (MPXG_00091 and MPXG_00148) had higher relative transcript abundances at T12 (4.6 and 2.0 fold change respectively) under low-P, consistent with the timing of large increases in free viral particles during the experiment. MPXG_00004 was the only viral gene that showed significant expressional differences at more than one time point (two-fold higher expression under low-P at T3 and T12; also enriched at T1.5, but not significantly), when comparing low-P and P-replete conditions. The function of the 692 aa protein encoded by MPXG_00004 is not known and this protein is not present in other prasinoviruses sequenced to date.

It is unclear whether some MpV-SP1 genes with unknown functions that were differentially expressed between replete- and low-P treatments have roles associated with P-acquisition or management, such as MPXG_00004. The only other whole transcriptome study focusing on viral expression under different phosphate conditions is on *Prochlorococcus* NATL2A and its cyanophage P-SSM2 (Lin *et al*., 2016). This study showed just two differentially expressed genes; both were upregulated under P starvation and are annotated as being involved in P-transport (the high-affinity phosphate-binding protein PSTS associated to a *pho* box-containing gene). Several prasinoviruses also encode phosphate transporters, specifically PHO4, which has been postulated to play a role in enhancing phosphate uptake by the host (Monier *et al*., 2012). However, MpV-SP1 does not encode this prasinophyte-derived phosphate transporter. MpV-SP1 was isolated off the southern coast of California (Cottrell and Suttle, 1991), an environment that is typically not considered P-limited, thus there is no *a priori* reason to expect that MpV-SP1 has adaptations that are specifically designed to deal with low-P.

More generally, a combination of lab and field studies, have suggested that viral production levels are limited when P-availability is low. Correlation analyses between phosphate concentration and viral abundance suggest of a strong link between these parameters (Finke *et al*., 2017a). Moreover, reduced burst size and a delayed lytic cycle have now been demonstrated under P depletion and nitrogen depletion for the prasinovirus that infects Clade C *Micromonas* strain LAC38 (Maat *et al*., 2014). Additionally, here we observe lower MpV-SP1 production by Clade D *M. pusilla* in the low-P treatment than in P-replete and in a different style of study, *E. huxleyi* lysis rates in nature appear to be higher in P-replete environments (Bratbak *et al*., 1996). However, the evolution of marine viruses, including MpV-SP1, are shaped by myriad factors, including the host genome, host dynamics and local environmental parameters that influence host growth and viral production. In turn, these presumably influence the retention of horizontally acquired genes in viruses and overall adaptation processes. Proteins that may provide viruses a selective advantage under P-limitation could be part of the pangenome (such as PHO4) of viruses that infect *M. pusilla* and these virus genotypes show differential distributions suggestive either of selection of viral genotypes in connection to environmental conditions (Finke *et al*., 2017b) or subtle differences in host strains present. However, differences in viral production associated with P-limited growth observed here (and in prior studies) are immutably intertwined with host growth rates, because they

Table 2. Members of the top-50 most expressed viral genes for which there is a known function

gene ID	putative function	functional category	FPKM average ± SD in P-replete
MPXG_00122	DNA polymerase IV	DNA replication	133,556 ± 30,454
MPXG_00082	mRNA guanylyltransferase	Transcription	76,072 ± 16,724
MPXG_00105	DNA ligase	DNA replication	29,998 ± 5,719
MPXG_00186	Exonuclease	DNA replication, Recombination	26,681 ± 5,269
MPXG_00059	DNA helicase	DNA replication	24,500 ± 3,307
MPXG_00202	transcription elongation factor	Transcription	24,426 ± 6,630
MPXG_00068	TATA-box binding protein	Transcription	21,652 ± 5,007
MPXG_00079	transcription initiation factor	Transcription	18,609 ± 3,424
MPXG_00080	Transcription factor OCT-1	Transcription	15,955 ± 5,125
MPXG_00057	RNAse III	Transcription	9,357 ± 1,744

Expression levels are based on FPKM values averaged over all time points. See Supplementary table S5 for overall viral expression data in both P treatments.

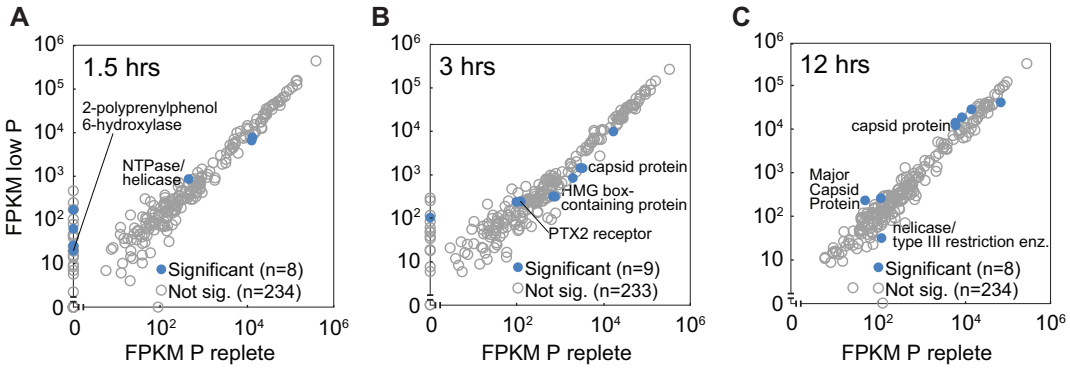

Fig. 4. Viral gene expression for infected cultures of P-replete (*x*-axis) and low-P (*y*-axis) acclimated *Micromonas*. Scatter plots represent FPKM for transcripts mapped to MpV-SP1 at (A) 1.5 h, (B) 3 h and (C) 12 h post-infection. Viral genes showing significant changes in relative transcript abundance between the two P treatments are denoted (blue), the ones with known function are labelled.

are also significantly different. Importantly, changes observed by RNA-seq in host machinery involved in transcription, ribosome biogenesis and translation, associated with the (different) treatments, point to the underlying cell biology that modulates host growth as the driver behind differences in viral production levels. In environments where phosphate availability differs to the extent of being nearly unavailable to the host, such as for *Prochlorococcus* in stratified Sargasso Sea conditions (Coleman and Chisholm, 2010), the limiting factor itself (phosphate) may play a greater role. Hence, the importance of phosphate availability in shaping viral evolution should be considered in a context-dependent manner.

While phosphate availability appeared to have a limited influence on expression of MpV-SP1 genes, there were strong temporal differences in the viral expressional profile. Forty-seven genes (19.4% of genes) were differentially expressed between at least two time points, under P-replete conditions (Fig. 5A). Fewer viral genes (14) showed differential expression under low-P (Fig. 5B), while the expression of 12 genes changed among time points under both P availability levels (Fig. 5, bold names). The transcript abundances for each of these genes revealed a strong temporal pattern over the course of the infection cycle, corresponding to T1.5 (Early), T3 (Intermediate) or T12 (Late), when expression was highest (Fig. 5). The gene MPXG-00072, which contains a thioredoxin domain, was an exception in that under P-replete conditions transcripts were detected at T1.5 and T12, but not at T3 (Fig. 5A). As above, the function of the majority of these genes is unknown. In the Early expressed cluster (green in Fig. 5A), two genes putatively code for proteins involved in DNA replication, including a DNA polymerase (MPXG_00122); two genes code for RING-containing domain proteins involved in protein synthesis, modification and degradation (MPXG_00070 and MPXG_00150), and one codes for transcription elongation factor SII (MPXG_00202). The Late expressed gene cluster (red in Fig. 5A) included two of eight genes coding for capsid proteins, which are essential for the assembly of new viral particles; other genes related to protein metabolism (MPXG_00003, MPXG_00107, MPXG_00230 and MPXG_00241) were also highly expressed in the Late cluster.

Temporal expression dynamics of the phycodnavirus PBCV-1, which infects the fresh water chlorophyte alga *Chlorella variabilis* (Etten *et al*., 1991) have been examined over a short time course (Yanai-Balser *et al*., 2010). While the temporal sampling of our experiment is very different from this prior study, global analysis of PBCV-1 expression using microarrays showed a temporal transcription pattern that also delineated into Early and Late expressed genes (Yanai-Balser *et al*., 2010). In another study, a subset of PBCV-1 genes were detected in the RNA-seq expression data as early as 7 minutes after infection (i.e., inoculation with the virus), and all viral genes were detected in RNA-seq data after 1 hour when sampling of the experiment was terminated (Blanc *et al*., 2014). Differences in timeframes examined, multiplicity of infections (MOI) and host-virus encounter rates, between our study and the *C. variabilis* infection experiments (Yanai-Balser *et al*., 2010; Blanc *et al*., 2014) limit possibilities for direct comparisons. However, as seen here, genes involved in replication, transcription and protein synthesis, modification and degradation, tended to show expression early, whereas genes related to viral structure (i.e., capsids) were expressed late.

Finally, differentially expressed viral genes in both P treatments tended to show the same temporal pattern of expression over the course of infection. For example, MPXG-00080, -00081 and -00200 had higher relative transcript abundances at T3, and MPXG-00125 was expressed early under both P-treatments. Identification of these temporal patterns will help future functional studies that involve either direct experimentation or comparison to other host-viral systems, as understanding of transcription and assembly of viral components deepens. Our results should facilitate analysis of metatranscriptomic studies that encounter viral infection events.

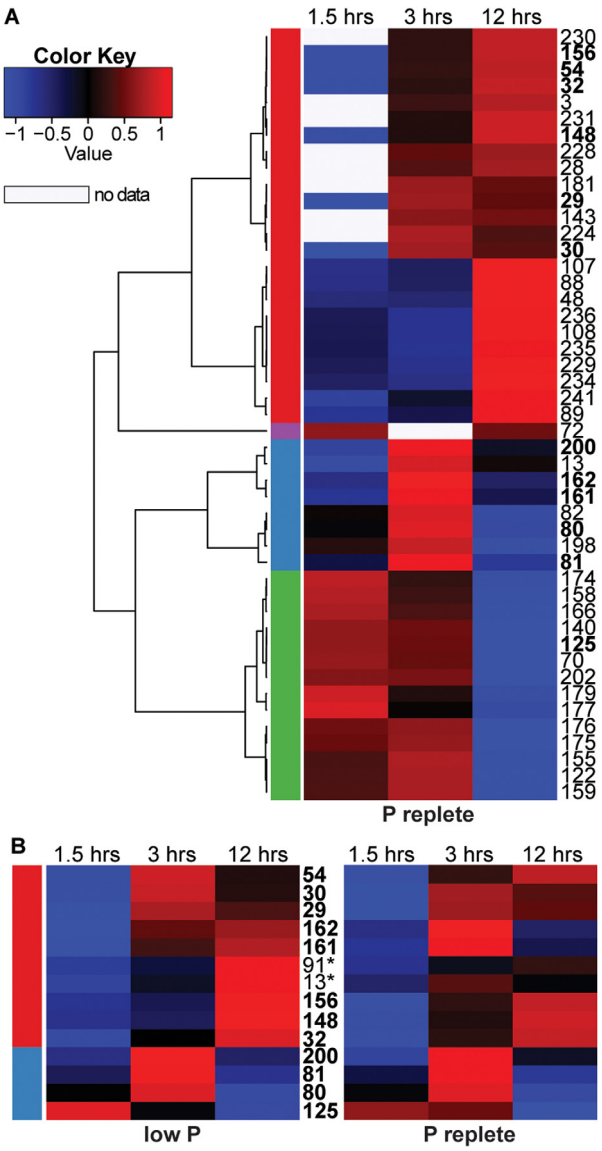

Fig. 5. Viral genes that were differentially expressed ($q < 0.01$ and FC > 1.5) between at least two time points in host cells acclimated to (A) P-replete and (B) low-P conditions (along with expression from P-replete for comparison). The $\log_2$ transformed *Z*-score (deviation from the mean transcript level across all time points and treatments for each respective gene) is shown with the direction of change indicated for negative (blue) or positive (red) for each gene across time points. For several genes no expression was detected (white) at one of the two earlier time points. Dendrograms of the hierarchical cluster analysis are shown on the left, with vertical bars (coloured) representing supported clusters (AU > 95%). Genes with asterisks were not significantly expressed in P-replete but shown in panel B to compare with low-P. *Y*-axis numbers are the gene locus tag as in NCBI and have the prefix MPXG_00 (followed by the number shown on *y*-axis).

Conclusion

Surface waters in the world oceans are predicted to become more stratified in the future, and consequently have lower nutrient availability (Behrenfeld *et al*., 2006; Capotondi *et al*., 2012). Hence, many algae may experience even wider fluctuations in nutrients, or more extreme nutrient limitation, in addition to the natural variations in nutrient availability that occur in today's marine ecosystems. Our results show that *M. pusilla* responds to P-deficiency through a specific and multi-faceted transcriptional makeover that allows it to maintain growth, albeit at a lower rate. We show that *M. pusilla* induces genes involved in high-affinity phosphate uptake, allocation of cellular P to polyphosphate, and phospholipid degradation that as a whole enhance acquisition of extracellular phosphorus and decrease cellular P demand. Importantly, we also report transcriptional changes in a unique set of genes that encode proteins with SLR-like domains. This protein family is greatly expanded in *M. pusilla* compared to members of other *Micromonas* clades and more distant prasinophytes, and therefore may reflect a species-specific adaptation to optimizing growth or competing under low-phosphate or other limiting nutrient conditions.

Marine host-virus-nutrient interactions are still understudied and to our knowledge this is the first study to characterize gene expression patterns of both a eukaryotic alga and its infecting virus, under differing nutrient conditions. The expression of genes encoded in the *M. pusilla* nuclear genome appears to be more strongly influenced by nutrient availability than by viral infection, at least under the environmentally relevant population infection percentages examined here. In contrast to the infected host gene profiles, transcription of MpV-SP1 genes showed a strong temporal program and only a few viral genes (most of unknown function) exhibited differential expression under the two phosphate conditions or different host growth rates induced by nutrient availability in our study. While these factors are immutably intertwined when the treatment (in this case low-P) induces massive changes in the population growth rate, our RNA-seq analyses, combined with results on viral production by N- and P-limited hosts (versus replete), suggest it is the cell biology behind modulation of host growth rate, rather than nutrient availability itself, that drives differences in viral production. Further, a primary host response to infection among known function gene transcripts appears to be enhancement of glycolysis, as also observed in animal-virus model systems and the haptophyte alga *E. huxleyi* when infected by EhV (Rosenwasser *et al*., 2014; Sanchez and Lagunoff, 2015; González Plaza *et al*., 2016). Notably, the strong signal for manipulation of host lipid metabolism observed during EhV infection (Rosenwasser *et al*., 2014) was not evident in our study. This underscores differences between strategies of evolutionarily distinct viral lineages, and the importance of characterizing relevant representative models for the broad array of marine host-virus systems. Collectively, our studies provide molecular-level insight into marine prasinoviruses that will facilitate future lab and field studies on infection dynamics and host-virus interactions.

Experimental procedures

Culturing and one-step infection experiment

Micromonas pusilla CCMP1545 (i.e. UTEX 991, Plymouth 27) was obtained from the Provasoli-Guillard National Center for Marine Algae and Microbiota (NCMA, East Boothbay, ME). Axenic cultures were grown in SESAWT, an artificial seawater medium (Cottrell and Suttle, 1991) based on ESAW (Harrison *et al*., 1980) that is modified by the addition of 5 mM Tris-HCl (pH 7.8) and selenium (10 nM). Cultures of *M. pusilla* were incubated at 19°C under continuous light at 232 μmol quanta m^{-2} s^{-1}. The experiment was set up to compare *M. pusilla* cells grown under replete conditions (P-replete) and conditions approaching limitation (low-P). Conditions under which phosphate was low or replete were established by altering the phosphate concentration (2.5 μM or 25 μM K_2HPO_4 respectively) and dilution (20% and 90% of μ_{max} respectively) of the cultures. Different growth rates were achieved by growing the cells in semi-continuous cultures, using daily dilution with fresh media (between 8 and 11 am and within 1 h from the previous day's dilution) for > 15 generations prior to the experiment start, following Suttle and Harrison (1986). The μ_{max} was calculated based on the average specific growth rate of *M. pusilla* cultures in exponential phase during preliminary experiments (0.76 d^{-1}, or 1.1 divisions per day). Preliminary experiments with batch cultures showed that 2.5 μM phosphate limited cell yield; whereas, 25 μM did not (data not shown).

On the day of the infection experiment, the low-P and P-replete cultures were diluted 50:50 with fresh medium and each split into six sub-cultures: three uninfected and three infected biological replicates. The MpV-SP1 stock used to inoculate experiments was prepared in 2.5 μM phosphate SESAWT media and filtered through a 0.45 μm HVLP 47 mm filter (Whatman) prior to use. The target MOI was approximately 10, with the goal of infecting 100% of the cells in the viral treatments. The volume of viral lysate added represented ~3.7% of the liquid volume of the *Micromonas* cultures. The abundance of *M. pusilla* cells at the time of viral addition was $4.0 \pm 0.2 \times 10^6$ and $3.6 \pm 0.9 \times 10^6$ ml^{-1} for the low-P and P-replete treatments respectively, based on flow cytometry counts (see Supporting Information Fig. S1). In the preliminary experiment ran with the same conditions, all replicates for both viral treatments had visually cleared by 48 hours.

Flow cytometry

Flow cytometry samples were collected at 0 h, 1.5 h, 3 h, 6 h, 12 h and 24 h and immediately fixed by adding 10 μl of 25% 0.45 μm filtered EM-grade glutaraldehyde to 490 μl of culture, incubating for 15 min at 4°C, and then flash freezing samples in liquid nitrogen. Samples were then stored at –80°C until analysis on a FACSCalibur (Becton-Dickinson, Franklin Lakes, New Jersey) after staining with SYBR Green for enumeration of viral particles (Payet and Suttle, 2008; Brussaard *et al*., 2010). The instrument was run at a nominal flow rate of 50 μl min.

RNA sampling and extraction

Cells from control (no virus added) and infected cultures were harvested 1.5, 3 and 12 h after viruses were added. At each time point samples for RNA extraction were collected by removing approximately 55 ml of culture in triplicate, gently filtering (34–48 kPa) through a 0.8 μm pore size 47 mm diameter Supor 800 filter (Pall Scientific, Port Washington, NY, USA) and immediately flash freezing in liquid nitrogen before storing at -80°C. RNA was extracted as described in (Duanmu *et al*., 2014). RNA integrity was evaluated on a 2100 Bioanalyzer (Agilent, Santa Clara, CA, USA) and quantity determined on a Qubit fluorometer (Thermo Fisher Scientific).

Transcriptome sequencing

Viral genes are expressed by the transcription machinery of host cells when they are infected, and host mRNA therefore contains transcripts of viral origin. Poly-adenylated RNA was isolated from 5 μg total RNA, extracted from each of two biological replicates, using the Dynabeads mRNA isolation kit (Thermo Fisher Scientific). The mRNA was purified, fragmented, reverse-transcribed and cDNA libraries prepared and sequenced as described in (Duanmu *et al*., 2014). Paired-end reads of 150 bp were generated using sequencing on the Illumina HiSeq platform. Between 46,506,281 and 78,703,685 reads were obtained per sample (average 56,375,249 per sample). Fewer reads (~9,000,000) were obtained for one biological replicate (the control low-P at T1.5 h, i.e., no virus added) with the RNA-seq and this sample was therefore excluded from the differential expression analysis. All data has been deposited in the SRA under NCBI BioProject PRJNA422663.

Differential expression analysis and hierarchical clustering

The experiments were performed and sequenced in triplicate; however, a robotic mishap resulted in sample destruction such that only duplicates could be analyzed for each treatment. Thus, RNA-seq from biological duplicates for each condition and time point (N = 24) were analyzed. The Tuxedo suite was used by first aligning reads to the respective genomes with gene models version of July 1, 2016 (*M. pusilla* and MpV-SP1 genomes, accessions NZ_ACCP01000000 and PRJNA47589 respectively) using TopHat version 1.4.0 (Trapnell *et al*., 2009) with

parameters -r 27 –mate-std-dev 100 –max-intron-length 10000 –min-intron-length 20 –library-type fr-firststrand. Gene level expression estimates in units of FPKM were calculated with Cuffnorm 2.2.1 (Trapnell *et al*., 2012) using quartile normalization (–library-norm-method quartile). For each sample, the number of host reads per gene was normalized among all libraries based on the total number of host-mapped reads in that sample. For each sample, the number of viral reads per gene was normalized based on the total number of viral mapped reads in that sample. Differentially expressed genes were identified using Cuffdiff 2.2.1 (Trapnell *et al*., 2013) to test the significant changes in relative transcript abundances between treatments from both the host and virus. All *q*-values provided have been False Discovery Rate (FDR)-corrected. The expression ratio between conditions for gene abundances was normalized as a $\log_2$ fold-change value. *Q*-values < 0.01 and fold-change values > 1.5 (i.e. 0.585 $\log_2$ fold-change) were both used to reflect statistically significant differences between low- and P-replete (T1.5 and T3 pooled together to increase statistical power from duplicates to quadruplicates) or between infected and non-infected host gene transcription, and between time points within P-treatments for viral gene transcription.

Cluster analyses, statistical computing and heat map visualization of viral gene expression profiles for genes showing significant differential expression between time points (T1.5 vs. T3, T3 vs. T12, T1.5 vs.T12) were performed as described in (Duanmu *et al*., 2014).

Finally, complete linkage hierarchical cluster analysis was performed on the Z scored transformed time series expression using the Pearson correlation as the distance matrix. We used pvclust (Suzuki and Shimodaira, 2006) for assessing the uncertainty in hierarchical cluster analysis where Approximatively Unbiased (AU) *p*-values are calculated via multiscale bootstrap resampling. Clusters strongly supported by the expression data (AU > 0.95) were identified.

Read counts and enrichment analysis

To compare the number of sequence reads assigned to viral or *M. pusilla* genomic features, we used HTSeq using a modified gff file comprising genome annotation information (Worden *et al*., 2009; van Baren *et al*., 2016) of the host and the virus (Anders *et al*., 2014). For the reads mapping to the virus genome, we assessed the percentage of nucleotides aligned to genes or intergenic regions using the Picard command line tool RnaSeqMetrics (http://broadinstitute.github.io/picard). Enrichment of KOG classes by differentially expressed genes was performed using gene set enrichment analysis (GSEA) (Subramanian *et al*., 2005). KOG classes with upregulated genes are displayed in supplementary tables and considered significantly enriched when FDR ≤ 0.05.

ACKNOWLEDGEMENTS

We are grateful to Alexander J. Limardo for help with RNA extractions, Amy E. Zimmerman for stimulating discussions, Govindarajan Kunde-Ramamoorthy for assistance, and Pam and Greg Landers for facilitating the first draft. This research was supported by NSERC, Canadian Foundation for Innovation (CFI), and BCKDF grants to CAS, a JGI Technology Development Project and funding from the David and Lucile Packard Foundation, the Gordon and Betty Moore Foundation (GBMF3788 and GBMF3305), NSF-IOS0843119 and DOE-DE-SC0004765 to AZW.

References

Adl, S.M., Simpson, A.G.B., Lane, C.E., Lukeš, J., Bass, D., and Bowser, S.S. (2012) The Revised Classification of Eukaryotes. *J Eukaryot Microbiol* **59**: 429–514.

Anders, S., Pyl, P.T., and Huber, W. (2014) HTSeq - A Python framework to work with high-throughput sequencing data. *bioRxiv* **00282**4.

van Baren, M.J., Bachy, C., Reistetter, E.N., Purvine, S.O., Grimwood, J., Sudek, S., *et al*. (2016) Evidence-based green algal genomics reveals marine diversity and ancestral characteristics of land plants. *BMC Genomics* **17**: 267.

Baudoux, A.-C., Lebredonchel, H., Dehmer, H., Latimier, M., Edern, R., Rigaut-Jalabert, F., *et al*. (2015) Interplay between the genetic clades of *Micromonas* and their viruses in the Western English Channel. *Environ Microbiol Rep* **7**: 765–773.

Behrenfeld, M.J., O'Malley, R.T., Siegel, D.A., McClain, C. R., Sarmiento, J.L., Feldman, G.C., *et al*. (2006) Climate-driven trends in contemporary ocean productivity. *Nature* **444**: 752–755.

Bellec, L., Clerissi, C., Edern, R., Foulon, E., Simon, N., Grimsley, N., and Desdevises, Y. (2014) Cophylogenetic interactions between marine viruses and eukaryotic picophytoplankton. *BMC Evol Biol* **14**: 59.

Bellec, L., Grimsley, N., Moreau, H., and Desdevises, Y. (2009) Phylogenetic analysis of new Prasinoviruses (Phycodnaviridae) that infect the green unicellular algae *Ostreococcus, Bathycoccus* and *Micromonas. Environ Microbiol Rep* **1**: 114–123.

Bender, S.J., Durkin, C.A., Berthiaume, C.T., Morales, R.L., and Armbrust, E.V. (2014) Transcriptional responses of three model diatoms to nitrate limitation of growth. *Aquat Microbiol* **1**: 3.

Blanc, G., Mozar, M., Agarkova, I.V., Gurnon, J.R., Yanai-Balser, G., Rowe, J.M., *et al*. (2014) Deep RNA sequencing reveals hidden features and dynamics of early gene transcription in *Paramecium bursaria Chlorella* Virus 1. *PLoS One* **9**: e90989.

Bratbak, G., Heldal, M., Thingstad, T.F., and Tuomi, P. (1996) Dynamics of virus abundance in coastal seawater. *FEMS Microbiol Ecol* **19**: 263–269.

Bratbak, G., Wilson, W., and Heldal, M. (1996) Viral control of *Emiliania huxleyi* blooms? *J Mar Syst* **9**: 75–81.

Brown, C.M., and Bidle, K.D. (2014) Attenuation of virus production at high multiplicities of infection in *Aureococcus anophagefferens*. *Virology* **466–467**: 71–81.

Brown, C.M., Campbell, D.A., and Lawrence, J.E. (2007) Resource dynamics during infection of *Micromonas pusilla* by virus MpV-Sp1. *Environ Microbiol* **9**: 2720–2727.

Brussaard, C.P., Payet, J.P., Winter, C., and Weinbauer, M. G. (2010) Quantification of aquatic viruses by flow cytometry. *Man Aquat Viral Ecol* **11**: 102–107.

Capotondi, A., Alexander, M.A., Bond, N.A., Curchitser, E. N., and Scott, J.D. (2012) Enhanced upper ocean stratification with climate change in the CMIP3 models. *J Geophys Res Oceans* **117**: C04031.

Caron, D.A., Alexander, H., Allen, A.E., Archibald, J.M., Armbrust, E.V., Bachy, C., *et al*. (2017) Probing the evolution, ecology and physiology of marine protists using transcriptomics. *Nat Rev Microbiol* **15**: 6–20.

Chen, F., and Suttle, C. (1996) Evolutionary relationships among large double-stranded DNA viruses that infect microalgae and other organisms as inferred from DNA polymerase genes. *Virology* **219**: 170–178.

Chung, C.-C., Hwang, S.-P.L., and Chang, J. (2003) Identification of a high-affinity phosphate transporter gene in a prasinophyte alga, *Tetraselmis chui*, and its expression under nutrient limitation. *Appl Environ Microbiol* **69**: 754–759.

Coleman, M.L., and Chisholm, S.W. (2010) Ecosystem-specific selection pressures revealed through comparative population genomics. *Proc Natl Acad Sci U S A* **107**: 18634–18639.

Cottrell, M.T., and Suttle, C.A. (1995) Dynamics of a lytic virus infecting the photosynthetic marine picoflagellate *Micromonas pusilla. Limnol Oceanogr* **40**: 730–739.

Cottrell, M.T., and Suttle, C.A. (1991) Wide-spread occurrence and clonal variation in viruses which cause lysis of a cosmopolitan, eukaryotic marine phytoplankter, *Micromonas pusilla. Mar Ecol Prog Ser* **78**: 1–9.

Culley, A.I., Asuncion, B.F., and Steward, G.F. (2009) Detection of inteins among diverse DNA polymerase genes of uncultivated members of the Phycodnaviridae. *ISME J* **3**: 409–418.

Cuvelier, M.L., Guo, J., Ortiz, A.C., Baren, MJ. V., Tariq, M. A., Partensky, F., and Worden, A.Z. (2017) Responses of the picoprasinophyte *Micromonas commoda* to light and ultraviolet stress. *PLoS One* **12**: e0172135.

Demory, D., Arsenieff, L., Simon, N., Six, C., Rigaut-Jalabert, F., Marie, D., *et al*. (2017) Temperature is a key factor in *Micromonas*–virus interactions. *ISME J* **11**: 601–612.

Derelle, E., Monier, A., Cooke, R., Worden, A.Z., Grimsley, N.H., and Moreau, H. (2015) Diversity of viruses infecting the green microalga Ostreococcus lucimarinus. *J Virol* **89**: 5812–5821.

Dörmann, P., and Benning, C. (2002) Galactolipids rule in seed plants. *Trends Plant Sci* **7**: 112–118.

Duanmu, D., Bachy, C., Sudek, S., Wong, C.-H., Jiménez, V., Rockwell, N.C., *et al*. (2014) Marine algae and land plants share conserved phytochrome signaling systems. *Proc Natl Acad Sci U S A* **111**: 15827–15832.

DuRand, M.D., Green, R.E., Sosik, H.M., and Olson, R.J. (2002) Diel variations in optical properties of *Micromonas pusilla* (prasinophyceae)1. *J Phycol* **38**: 1132–1142.

Dyhrman, S.T., Haley, S.T., Birkeland, S.R., Wurch, L.L., Cipriano, M.J., and McArthur, A.G. (2006) Long serial analysis of gene expression for gene discovery and transcriptome profiling in the widespread marine coccolithophore *Emiliania huxleyi. Appl Environ Microbiol* **72**: 252–260.

Dyhrman, S.T., Jenkins, B.D., Rynearson, T.A., Saito, M.A., Mercier, M.L., Alexander, H., *et al*. (2012) The transcriptome and proteome of the diatom *thalassiosira pseudonana* reveal a diverse phosphorus stress response. *PLoS One* **7**: e33768.

Etten, J.L.V., Lane, L.C., and Meints, R.H. (1991) Viruses and virus-like particles of eukaryotic algae. *Microbiol Rev* **55**: 586–620.

Field, C., Behrenfeld, M., Randerson, J., and Falkowski, P. (1998) Primary production of the biosphere: integrating terrestrial and oceanic components. *Science* **281**: 237–240.

Finke, J.F., Hunt, B.P.V., Winter, C., Carmack, E.C., and Suttle, C.A. (2017a) Nutrients and other environmental factors influence virus abundances across oxic and hypoxic marine environments. *Viruses* **9**: 152.

Finke, J.F., Winget, D.M., Chan, A.M., and Suttle, C.A. (2017b) Variation in the genetic repertoire of viruses infecting *Micromonas pusilla* reflects horizontal gene transfer and links to their environmental distribution. *Viruses* **9**: 116.

González Plaza, J.J., Hulak, N., Kausova, G., Zhumadilov, Z., and Akilzhanova, A. (2016) Role of metabolism during viral infections, and crosstalk with the innate immune system. *Intractable Rare Dis Res* **5**: 90–96.

Grossman, A.R., and Aksoy, M. (2015) Algae in a phosphorus-limited landscape. In *Annual Plant Reviews, Vol. 48*. Plaxton, W.C. and Lambers, H. (eds). Hoboken, New Jersey: Wiley, pp. 337–374.

Guillou, L., Eikrem, W., Chrétiennot-Dinet, M.-J., Le Gall, F., Massana, R., Romari, K., *et al*. (2004) Diversity of picoplanktonic prasinophytes assessed by direct nuclear SSU rDNA sequencing of environmental samples and novel isolates retrieved from oceanic and coastal marine ecosystems. *Protist* **155**: 193–214.

Guo, J., Wilken, S., Jimenez, V., Choi, C.J., Ansong, C., Dannebaum, R., *et al*. (2018) Specialized proteomic responses and an ancient photoprotection mechanism sustain marine green algal growth during phosphate limitation. *Nat Microbiol* **3**: 781–790.

Hanson, G., and Coller, J. (2018) Codon optimality, bias and usage in translation and mRNA decay. *Nat Rev Mol Cell Biol* **19**: 20–30.

Harrison, P.J., Waters, R.E., and Taylor, F.J.R. (1980) A broad spectrum artificial sea water medium for coastal and open ocean phytoplankton. *J Phycol* **16**: 28–35.

Jacquet, S., Partensky, F., Lennon, J., and Vaulot, D. (2001) Diel patterns of growth and division in marine picoplankton in culture. *J Phycol* **37**: 357–369.

Jover, L.F., Effler, T.C., Buchan, A., Wilhelm, S.W., and Weitz, J.S. (2014) The elemental composition of virus particles: implications for marine biogeochemical cycles. *Nat Rev Microbiol* **12**: 519–528.

Keeling, P.J., Burki, F., Wilcox, H.M., Allam, B., Allen, E.E., Amaral-Zettler, L.A., *et al*. (2014) The Marine Microbial Eukaryote Transcriptome Sequencing Project (MMETSP): illuminating the functional diversity of eukaryotic life in the oceans through transcriptome sequencing. *PLoS Biol* **12**: e1001889.

Kelly, L., Ding, H., Huang, K.H., Osburne, M.S., and Chisholm, S.W. (2013) Genetic diversity in cultured and

wild marine cyanomyoviruses reveals phosphorus stress as a strong selective agent. *Isme J* **7**: 1827–1841.

King, A.M.Q., Adams, M.J., Lefkowitz, E.J., and Carstens, E. B. (2012) *Virus Taxonomy: Classification and Nomenclature of Viruses: Ninth Report of the International Committee on Taxonomy of Viruses*. New York, NY: Elsevier.

Lin, X., Ding, H., and Zeng, Q. (2016) Transcriptomic response during phage infection of a marine cyanobacterium under phosphorus-limited conditions. *Environ Microbiol* **18**: 450–460.

Maat, D.S., Bale, N.J., Hopmans, E.C., Sinninghe Damsté, J.S., Schouten, S., and Brussaard, C.P.D. (2016a) Increasing P limitation and viral infection impact lipid remodeling of the picophytoplankter *Micromonas pusilla. Biogeosciences* **13**: 1667–1676.

Maat, D.S., van Bleijswijk, J.D.L., Witte, H.J., and Brussaard, C. P.D. (2016b) Virus production in phosphorus-limited *Micromonas pusilla* stimulated by a supply of naturally low concentrations of different phosphorus sources, far into the lytic cycle. *FEMS Microbiol Ecol* **92**: fiw136.

Maat, D.S., de Blok, R., and Brussaard, C.P.D. (2016c) Combined phosphorus limitation and light stress prevent viral proliferation in the phytoplankton species *Phaeocystis globosa*, but not in *Micromonas pusilla*. *Aquat Microbiol* 160.

Maat, D.S., and Brussaard, C.P.D. (2016) Both phosphorus- and nitrogen limitation constrain viral proliferation in marine phytoplankton. *Aquat Microb Ecol* **77**: 87–97.

Maat, D.S., Crawfurd, K.J., Timmermans, K.R., and Brussaard, C.P.D. (2014) Elevated CO2 and phosphate limitation favor *Micromonas pusilla* through stimulated growth and reduced viral impact. *Appl Environ Microbiol* **80**: 3119–3127.

Martínez Martínez, J., Boere, A., Gilg, I., Lent, V. JWM., Witte, H.J., van Bleijswijk, JDL., and Brussaard, C.P.D. (2015) New lipid envelop-containing dsDNA virus isolates infecting *Micromonas pusilla* reveal a separate phylogenetic group. *Aquat Microb Ecol* **74**: 17–28.

Massana, R. (2011) Eukaryotic picoplankton in surface oceans. *Annu Rev Microbiol* **65**: 91–110.

Mayer, J.A., and Taylor, F.J.R. (1979) A virus which lyses the marine nanoflagellate *Micromonas pusilla. Nature* **281**: 299–301.

Minnikin, D.E., Abdolrahimzadeh, H., and Baddiley, J. (1974) Replacement of acidic phospholipids by acidic glycolipids in *Pseudomonas diminuta. Nature* **249**: 268–269.

Mittl, P.R.E., and Schneider-Brachert, W. (2007) Sel1-like repeat proteins in signal transduction. *Cell Signal* **19**: 20–31.

Monier, A., Chambouvet, A., Milner, D.S., Attah, V., Terrado, R., Lovejoy, C., *et al*. (2017) Host-derived viral transporter protein for nitrogen uptake in infected marine phytoplankton. *Proc Natl Acad Sci U S A* **114**: E7489–E7498.

Monier, A., Welsh, R.M., Gentemann, C., Weinstock, G., Sodergren, E., Armbrust, E.V., *et al*. (2012) Phosphate transporters in marine phytoplankton and their viruses: cross-domain commonalities in viral-host gene exchanges. *Environ Microbiol* **14**: 162–176.

Moniruzzaman, M., LeCleir, G.R., Brown, C.M., Gobler, C.J., Bidle, K.D., Wilson, W.H., and Wilhelm, S.W. (2014) Genome of brown tide virus (AaV), the little giant of the Megaviridae, elucidates NCLDV genome expansion and host–virus coevolution. *Virology* **466–467**: 60–70.

Moreau, H., Piganeau, G., Desdevises, Y., Cooke, R., Derelle, E., and Grimsley, N. (2010) Marine prasinovirus genomes show low evolutionary divergence and acquisition of protein metabolism genes by horizontal gene transfer. *J Virol* **84**: 12555–12563.

Oh, Y., Schreiter, J.H., Okada, H., Wloka, C., Okada, S., Yan, D., *et al*. (2017) Hof1 and Chs4 Interact via F-BAR Domain and Sel1-like Repeats to Control Extracellular Matrix Deposition during Cytokinesis. *Curr Biol* **27**: 2878–2886.

Orchard, E.D., Webb, E.A., and Dyhrman, S.T. (2009) Molecular analysis of the phosphorus starvation response in *Trichodesmium* spp. *Environ Microbiol* **11**: 2400–2411.

Payet, J.P., and Suttle, C.A. (2008) Physical and biological correlates of virus dynamics in the southern Beaufort Sea and Amundsen Gulf. *J Mar Syst* **74**: 933–945.

Rosenwasser, S., Mausz, M.A., Schatz, D., Sheyn, U., Malitsky, S., Aharoni, A., *et al*. (2014) Rewiring host lipid metabolism by large viruses determines the fate of *Emiliania huxleyi*, a bloom-forming alga in the ocean. *Plant Cell Online* tpc.114.125641.

Sanchez, E.L., and Lagunoff, M. (2015) Viral activation of cellular metabolism. *Virology* **479–480**: 609–618.

Schachtman, D.P., Reid, R.J., and Ayling, S.M. (1998) Phosphorus uptake by plants: From soil to cell. *Plant Physiol* **116**: 447–453.

Simmons, M.P., Bachy, C., Sudek, S., Baren, MJ. V., Sudek, L., Ares, M., and Worden, A.Z. (2015) Intron invasions trace algal speciation and reveal nearly identical Arctic and Antarctic *Micromonas* populations. *Mol Biol Evol* **32**: 2219–2235.

Simon, N., Foulon, E., Grulois, D., Six, C., Desdevises, Y., Latimier, M., *et al*. (2017) Revision of the genus *Micromonas* manton et parke (Chlorophyta, Mamiellophyceae), of the type species *M. pusilla* (Butcher) Manton & Parke and of the Species M. commoda van Baren, Bachy and Worden and Description of Two New Species Based on the Genetic and Phenotypic Characterization of Cultured Isolates. *Protist* **168**: 612–635.

Šlapeta, J., López-García, P., and Moreira, D., (2006) Global dispersal and ancient cryptic species in the smallest marine eukaryotes. *Mol Biol Evol* **23**: 23–29.

Subramanian, A., Tamayo, P., Mootha, V.K., Mukherjee, S., Ebert, B.L., Gillette, M.A., *et al*. (2005) Gene set enrichment analysis: a knowledge-based approach for interpreting genome-wide expression profiles. *Proc Natl Acad Sci U S A* **102**: 15545–15550.

Sullivan, M.B., Coleman, M.L., Weigele, P., Rohwer, F., and Chisholm, S.W. (2005) Three Prochlorococcus cyanophage genomes: signature features and ecological interpretations. *PLoS Biol* **3**: e144.

Suttle, C.A., and Harrison, P.J. (1986) Phosphate uptake rates of phytoplankton assemblages grown at different dilution rates in semicontinuous culture. *Can J Fish Aquat Sci* **43**: 1474–1481.

Suzuki, R., and Shimodaira, H. (2006) Pvclust: an R package for assessing the uncertainty in hierarchical clustering. *Bioinformatics* **22**: 1540–1542.

Trapnell, C., Hendrickson, D.G., Sauvageau, M., Goff, L., Rinn, J.L., and Pachter, L. (2013) Differential analysis of gene regulation at transcript resolution with RNA-seq. *Nat Biotechnol* **31**: 46–53.

Trapnell, C., Pachter, L., and Salzberg, S.L. (2009) TopHat: discovering splice junctions with RNA-Seq. *Bioinformatics* **25**: 1105–1111.

Trapnell, C., Roberts, A., Goff, L., Pertea, G., Kim, D., Kelley, D.R., *et al*. (2012) Differential gene and transcript expression analysis of RNA-seq experiments with TopHat and Cufflinks. *Nat Protoc* **7**: 562–578.

Treusch, A.H., Demir-Hilton, E., Vergin, K.L., Worden, A.Z., Carlson, C.A., Donatz, M.G., *et al*. (2012) Phytoplankton distribution patterns in the northwestern Sargasso Sea revealed by small subunit rRNA genes from plastids. *ISME J* **6**: 481–492.

Van Mooy, B.A.S., Fredricks, H.F., Pedler, B.E., Dyhrman, S.T., Karl, D.M., Koblížek, M., *et al*. (2009) Phytoplankton in the ocean use non-phosphorus lipids in response to phosphorus scarcity. *Nature* **458**: 69–72.

Waltman, P.H., Guo, J., Reistetter, E.N., Purvine, S., Ansong, C. K., van Baren, M.J., *et al*. (2016) Identifying aspects of the post-transcriptional program governing the proteome of the green alga *Micromonas pusilla. PLoS One* **11**: e0155839.

Waters, R.E., and Chan, A.T. (1982) *Micromonas pusilla* virus: the virus growth cycle and associated physiological events within the host cells; host range mutation. *J Gen Virol* **63**: 199–206.

Whitney, L.P., and Lomas, M.W. (2016) Growth on ATP elicits a P-stress response in the picoeukaryote *Micromonas pusilla. PLoS One* **11**: e0155158.

Wilson, W.H., Carr, N.G., and Mann, N.H. (1996) The effect of phosphate status on the kinetics of cyanophage infection in the oceanic cyanobacterium *Synechococcus* Sp. Wh78031. *J Phycol* **32**: 506–516.

Worden, A.Z. (2006) Picoeukaryote diversity in coastal waters of the Pacific Ocean. *Aquat Microb Ecol* **43**: 165–175.

Worden, A.Z., Lee, J.-H., Mock, T., Rouzé, P., Simmons, M. P., Aerts, A.L., *et al*. (2009) Green evolution and dynamic adaptations revealed by genomes of the marine picoeukaryotes Micromonas. *Science* **324**: 268–272.

Worden, A.Z., and Not, F. (2008) Ecology and diversity of picoeukaryotes. In *Microbial Ecology of the Oceans* Kirchman, D.L. (ed.). Hoboken, New Jersey: Wiley, pp. 159–205.

Wurch, L.L., Bertrand, E.M., Saito, M.A., Mooy, B.A.S.V., and Dyhrman, S.T. (2011) Proteome changes driven by phosphorus deficiency and recovery in the brown tide-forming alga *Aureococcus anophagefferens. PLoS One* **6**: e28949.

Wurch, L.L., Gobler, C.J., and Dyhrman, S.T. (2014) Expression of a xanthine permease and phosphate transporter in cultures and field populations of the harmful alga *Aureococcus anophagefferens*: tracking nutritional deficiency during brown tides. *Environ Microbiol* **16**: 2444–2457.

Yanai-Balser, G.M., Duncan, G.A., Eudy, J.D., Wang, D., Li, X., Agarkova, I.V., *et al*. (2010) Microarray Analysis of *Paramecium bursaria Chlorella* Virus 1 Transcription. *J Virol* **84**: 532–542.

Zeng, Q., and Chisholm, S.W. (2012) Marine viruses exploit their host's two-component regulatory system in response to resource limitation. *Curr Biol* **22**: 124–128.

Supporting Information

Additional Supporting Information may be found in the online version of this article at the publisher's web-site:

Fig. S1. Flow cytometric quantification and characterization of the alga *M. pusilla.*

A. *M. pusilla* exhibited unsynchronized division under continuous light, as expected, and as manifested by the linear increase in cell numbers (as opposed to punctuated 'jumps' in cell numbers reflected by synchronized M. commoda cultures, see Cuvelier *et al*., 2017). In both P-treatments cells increased relatively constantly, in a linear manner over time, relative change from T0, but more so in the replete cultures (demonstrating faster growth of replete cells than those in the low phosphate treatment). Note that growth rate of the P-replete culture slowed between T12 and T24 relative to that between T0 and T12 or the pre-experiment culture, potentially due to the amount of fresh-medium added at the start being inadequate for the cell concentration used; this time point was not used for expression analyses.

B. Cell size (represented as bead-normalized mean forward angle light scatter, FALS) is constant throughout the experiment period from T0 to T12 and does not exhibit the diel variations that are observed during light:dark synchronized *Micromonas* cell division (see Jacquet *et al*., 2001; Duanmu *et al*., 2014; Cuvelier *et al*., 2017). Cells acclimated to low P conditions exhibit higher FALS than P-replete due to the fact that slower growing cells are larger (fewer cells divide and a greater proportion are suspended in G2/larger cell size) than for faster growing cells, at least based on studies of light-limited growth (Cuvelier *et al*., 2017). The increased FALS at T24 for the replete treatment is consistent with the observed reduction in growth rate that occurred between T12 and T24.

Fig. S2. Flow cytometric quantification and characterization of the *M. pusilla* free-chloroplasts.

Fig. S3. Distribution of reads mapped on the MpV-SP1 genome. The plain bar is the number of reads mapped to the MpV-SP1 genome and the faint bar is the percentage of the total reads that map to the MpV-SP1 genome. T-tests between levels of P show significance for each time point (*, above P replete bars represent significance for comparisons with low P).

Table S1. List of *Micromonas* nuclear encoded genes showing significant differences ($q < 0.01$ and FC>1.5) in pairwise normalized FPKM comparisons between P-replete and low-P conditions (quadriplicates for each condition with T1.5 and T3 pooled together). The SLR genes are in bold.

Table S2. Upper quartile normalized FPKM for the *Micromonas* nuclear genome encoded genes. Values represent the average of biological duplicates in all phosphate treatments and time points for uninfected and infected cells.

Table S3. Reports of the enrichment analyses for different conditions showing significantly differentially expressed gene sets for all analyses displayed in Fig. 3.

Table S4. List of *Micromonas* nuclear encoded genes showing significant differences ($q < 0.01$ and FC > 1.5) in pairwise normalized FPKM comparisons between uninfected and infected cells (T12).

Table S5. Upper quartile normalized FPKM for the MpV-SP1 viral genome encoded genes. Values represent the average of biological duplicates in all phosphate treatments and time points for infected cells.